

A Novel Technique for Human Traffic based Radio Map Updating in Wi-Fi Indoor Positioning Systems

Yun Mo^{1,2,3}, Zhongzhao Zhang^{1,2}, Yang Lu¹, and Gul Agha³

1 Communication Research Center, Harbin Institute of Technology, Harbin 150080, China
[e-mail: zzzhang@hit.edu.cn]

2 Key Laboratory of Police Wireless Digital Communication, Ministry of Public Security, Harbin 150080, China
[e-mail: zzzhang@hit.edu.cn]

3 Open System Laboratory, University of Illinois at Urbana-Champaign, Champaign, IL 61801, USA
[e-mail: agha@illinois.edu]

*Corresponding author: ZhongZhao Zhang

Received *January 7, 2015*; revised *April 7, 2015*; accepted *May 3, 2015*;
published *May 31, 2015*

Abstract

With the fast-developing of mobile terminals, positioning techniques based on fingerprinting method draws attention from many researchers even world famous companies. To conquer some shortcomings of the existing fingerprinting systems and further improve its performance, we propose a radio map building and updating technique, which is able to customize the spatial and temporal dependency of radio maps. The method includes indoor propagation and penetration modeling and the analysis of human traffic. Based on the combination of Ray-Tracing Algorithm, Finite-Different Time-Domain and Rough Set Theory, the approach of indoor propagation modeling accurately represents the spatial dependency of the radio map. In terms of temporal dependency, we specifically study the factor of moving people in the interest area. With measurement and statistics, the factor of human traffic is introduced as the temporal updating component. We improve our existing indoor positioning system with the proposed building and updating method, and compare the localization accuracy. The results show that the enhanced system can conquer the influence caused by moving people, and maintain the confidence probability stable during week, which enhance the actual availability and robustness of fingerprinting-based indoor positioning system.

Keywords: radio map building, updating, indoor propagation modeling, human traffic

1. Introduction

With the fast-developing of mobile terminals and wireless network techniques, Location Based Services (LBS) are becoming unprecedented popular recent years. World prestigious research institutions have exerted great attention and effort on both indoor positioning and relative business applications, such as the cooperation between Alibaba and AutoNavi, the competition between Google and Baidu. Many emerging indoor positioning systems based on ultrasound, infrared and radio frequency have been proposed recently [1, 2]. Fingerprinting method, as one of the most convenient techniques, has exhibited more popularity than other systems in the application of civilian uses due to its capability of using the existing WLAN infrastructure and its wide coverage [3, 4].

Besides the convenience, nevertheless, the finger printing based positioning system extremely requires accurate information of the radio maps. There are many methods to build radio maps, typically including construction based on measured received signal strength (RSS) values and prediction based on signal propagation or a combination of both [5-8]. Measurement based methods are very time-consuming and include exhaustive measurement campaigns to collect finger prints at all the locations of the interesting environment. Moreover, the lack of robustness about temporal changes in the environment directly affects the RSS values, which may significantly affect the positioning performance.

In this paper, considering the spatial and temporal dependency of radio maps, we propose a technique including building and updating radio maps for positioning in indoor environments. The building method is based on the combination of ray-tracing algorithm (RTA), finite-difference time-domain (FDTD) technique and rough set theory (RST), which efficiently balance the model accuracy and computation complexity. For the updating process, considering the limited influence of opening and closing doors (and windows) in addition to little chance of facilities removing, we mainly focus on the human traffic influence instead of updating whole radio map continuously and repeatedly. Actually it is the key variation factor significantly interferes indoor environments.

We have done some research works on indoor positioning systems [9, 10] and green clustering methods [11, 12], where we analyzed the related technologies, built the experiment environments and realize the system on Android based terminal. In this paper, we mainly focus on the radio map building and updating process which is a significant supplementary component of the proposed system, because it may boost the system generalization and enhance the robustness. The remainder of this paper is organized as follows. In Section 2, we review the previous work in building and updating radio maps. Section 3 proposes an indoor propagation and penetration modeling method based on the combination of RTA, FDTD and RST. We analyze and introduce the factor of moving people as the temporal component in the updating process, and allocate the corresponding implement in Section 4. Conclusion is remarked in Section 5.

2. Related Work

In terms of radio map building, Reference [13] proposed a scheme based on inertial sensors of smart phone. Despite of the unmanageable sensor cumulative error, it is an effective and practical method for updating radio map in relatively crowded environment. Although

automatically cooperating and uploading RSS data when serving by terminals in network is labor-saving, this method is measurement-based and therefore lacks robustness of temporal changes in the environment, even malfunctions on locations where few people move. In [14], authors introduce a radio map building method by an RTA based software (3DTruEM) and employs different terminals for calibration, which verified the availability of radio map building based on simulated propagation model without (or with few) actual measurement. But this modeling method seems can be enhanced according to the given positioning results.

Some works have proposed algorithms to solve the problem of variations of RSS radio maps between different times using limited calibration, such as LANDMARK [15], LEASE [16], LEMT [17] and LuMA [18]. All these techniques require a complete and accurate radio map as the basis, and the accumulation of information adaption during updating may also increase the localization error. In [19], a radio map generation with its updating solution based on modeling simulator (VLAB) and crowd-sourced unlabeled measurement is proposed with a limited number of labeled fingerprinting calibration. Lim et.al, use the feedback data for update, and the temporal dependency of radio maps is proposed and considered in the system [20]. Similar with it, in [21], a radio map for indoor positioning is set up during the calibration phase, and RSS samples at each point are recorded and converted into a probability density function for positioning. Reference [22] proposes an environment-specific radio map management method, where different features of signal propagation are obtained in different regions of the indoor positioning area. The entire environment is reasonably divided based on the different features, and the RSS values collected at the trained locations in different regions will be updated according those features. However, the researches above focus on the updating techniques but pay less attention on the environment variation factors. In addition, continuously updating radio map may cause accumulative error and huge computational burden.

Actually in a relatively developed environment, besides the limited influence of doors, windows and removed facilities, moving people is the most significant feature as the temporal component in an indoor positioning system. Furthermore, the amount of moving people normally would show a regular varying pattern, which is supposed to be well utilized. Therefore, based on the proved availability of propagation model for positioning and our previously proposed indoor localization system, we present a novel indoor propagation and penetration model efficiently combined with Ray-Tracing, FDTD and Rough Set Theory for radio map building, and effectively deploy the moving people factor for radio map updating process.

3. Indoor Propagation and Penetration Analysis Approach Based on Ray-Tracing, FDTD and Rough Set

Fingerprinting indoor positioning systems, in most cases, may suffer less from the signal penetration and propagation complexity in an indoor environment, which means it may be more applicable to complex indoor environments than some of others in an economical way. Actually it is based on databases consisting of RSS recorded from APs, namely radio map. Different from TOA, TDOA and AOA, signal analysis generally do not participate location estimation process in the fingerprinting method, but calculation of RSS or the radio map building, as the key database generating process, in fact plays a significant role in the whole positioning system.

However, the approaches to generate such a database are mainly derived from actual measurement or modeling simulation. Referring to measurement, which most radio maps in the existed indoor positioning systems proposed by literatures are based on, the timeliness is limited. And the process of radio map building by means of measurement is highly time-consuming. Indeed, it is a hard work but with limited robustness that makes the generalization poor as well. Some researches build the radio map by simulation modeling software VLAB and 3DTrueEM, though availability can be validated, the positioning performance need to be further improved. Therefore, we propose an enhanced simulation modeling method, which is based on the combination of ray-tracing algorithm, FDTD technique and rough set theory, to build the radio map in an efficient way.

3.1 The Combination of Ray-Tracing and FDTD

Ray-tracing method is presented to evaluate the indoor wave propagation and penetration. According to ray-tracing, waves from a Tx antenna could be modeled as ray tubes, and from geometrical optics, the E-field of the ray tube at Rx can be given by

$$\vec{E} = \vec{E}_0 \cdot \left\{ \prod \vec{\bar{R}}_i \right\} \cdot \left\{ \prod \vec{\bar{T}}_i \right\} \cdot \left\{ \prod \exp(-\gamma_i l_i) \right\} \cdot SF \quad (1)$$

where \vec{E}_0 denotes the E-field at a reference point RP_0 , $\left\{ \prod \vec{\bar{R}}_i \right\}$ and $\left\{ \prod \vec{\bar{T}}_i \right\}$ represent the reflection and transmission coefficient dyads along the whole path, respectively. $\left\{ \prod \exp(-\gamma_i l_i) \right\}$ denotes the propagation phase variations and exponential losses for the ray contribution from RP_0 . Both γ_i and l_i would be derived from dielectric properties (in 2.4GHz spectrum) of the building materials, where the materials are indicated in the blueprint and the propagation constants are verified by the material property measurements. In terms of the given environment, only the major effects of the structures were considered in the experiment, and complex dielectric constants were used empirically in the propagation constants so that low lossy materials such as concrete and brick walls may be simulated and E-field function could be calculated. Forming the conservation of energy flux in a ray tube, SF can be obtained as

$$SF = \sqrt{A_0/A} \quad (2)$$

where A_0 and A are the cross-sectional areas at RP_0 and the filed point, respectively.

FDTD is present by Kane Yee for numerical solution of Maxwell's Equations. In FDTD, a space grid is introduced in which E-field components and H-field components at different directions are discretized, so each E-field component is encircled by four H-field components, and also each H-field component is encircled by four E-field components. And in time domain, both E-field and H-field components are also discretized arranging at regular intervals. According to FDTD, in a 3-D scenario, for instance, E-field component at direction x E_x can be given by

$$\begin{aligned}
E_x|_{i,j+1/2,k+1/2}^{n+1/2} &= \left(\frac{1 - \frac{\sigma_{i,j+1/2,k+1/2}\Delta t}{2\varepsilon_{i,j+1/2,k+1/2}}}{1 + \frac{\sigma_{i,j+1/2,k+1/2}\Delta t}{2\varepsilon_{i,j+1/2,k+1/2}}} \right) E_x|_{i,j+1/2,k+1/2}^{n-1/2} \\
&+ \left(\frac{\frac{\Delta t}{\varepsilon_{i,j+1/2,k+1/2}}}{1 + \frac{\sigma_{i,j+1/2,k+1/2}\Delta t}{2\varepsilon_{i,j+1/2,k+1/2}}} \right) \cdot \left(\frac{H_z|_{i,j+1,k+1/2}^n - H_z|_{i,j,k+1}^n}{\Delta y} - \frac{H_y|_{i,j+1/2,k+1}^n - H_y|_{i,j+1/2,k}^n}{\Delta z} - J_{SOURCE_x}|_{i,j+1/2,k+1/2}^n \right)
\end{aligned} \quad (3)$$

where n denotes time, ε and σ are material constants, E and H represent values of E- and H-field, respectively, and propagation directions of electromagnetic waves are denoted by x, y and z in a rectangular coordinate system. Δx , Δy and Δz are space increments in Yee grid, i , j and k are parameters to describe distances at direction x, y, and z, respectively. Δt is the time increment. Analogously, components E_y , E_z , H_x , H_y and H_z can be obtained with Yee grid through FDTD technology. Therefore, with previous time field, another field at adjacent nodes, electric and magnetic current sources, values of E- and H-field can be achieved at arbitrary point in Yee grid.

However, in FDTD, the space grid size must be a fraction of the wavelength for ensuring that over one increment the EM field does not change significantly. That means to model indoor wave propagation in a larger area could be very difficult using existing equipment and the computation amount would be huge. For balancing exactness and feasibility, a combination of ray-tracing and FDTD is introduced for indoor positioning environment.

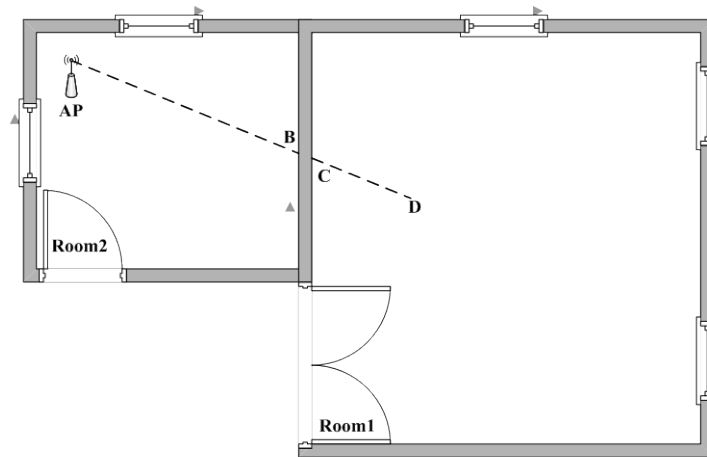


Fig. 1. Illustration of modeling indoor wave propagation.

In a scenario illustrated by **Fig. 1**, which is a typical indoor environment, the wave propagation between AP and Location D is concerned. A combination of ray-tracing and FDTD is that the propagation between AP and B, C and D is estimated based on ray-tracing method, and the propagation between B and C is calculated based on FDTD method, similarly with the method proposed in [23]. Every wall of the building is discretized into a unit cell

(brick), Tx and Rx are added. The interaction between Tx and the bricks can be calculated iteratively according to (4), (5) and (6), and to simplify the explanation, vertical polarization with the three field components E_z , H_x and H_y is assumed. The derivation for horizontal polarization is analogous.

$$\vec{E} = \frac{\omega\mu I_0}{4} H_0^{(2)}(k|\vec{r} - \vec{r}'|) \bullet \hat{z} \quad (4)$$

where $H_0^{(2)}$ is the Hankel function of second kind, \vec{r} and \vec{r}' denote the vectors to Tx and to the brick point, respectively. k is the wave number.

$$\vec{M}_s = 2\vec{E}_s \times \vec{n} \quad (5)$$

where $\vec{E}_s = E_s \hat{z}$ are the electric surfaces fields in the z-direction, and \vec{n} is the surface normal vector of the brick.

$$\vec{E} = \frac{k}{4j} \bullet \int 2E_s \bullet H_0^{(2)'}(k|\vec{r} - \vec{r}'|) \bullet \frac{\vec{n} \bullet |\vec{r} - \vec{r}'|}{|\vec{r} - \vec{r}'|} dl \bullet \hat{z} \quad (6)$$

The analogous combinations of ray-tracing and FDTD have already been proved in [23-25], and the analogous implementations have been achieved in our previous work [11, 12].

3.2 Data Completing Technique based on RST

Although the solution of Maxwell's Equations can be achieved by means of FDTD technique, the solving process is highly time-consuming, in particular when applied in a large scale area. The Ray-Tracing algorithm (RTA), therefore, is introduced as a compromised solution. However, the building process of radio map used in an indoor positioning system requires a relatively short time, especially in updating process. The combination approach of RTA and FDTD is relatively time-saving, however, it might not meet the desired timeliness some times. Thus, further improvement of the indoor modeling method is necessary. To address the issue of timeliness, aiming at the calculating reduction, we introduce a data completing technique based on rough set theory (RST).

To build a radio map, we mesh the WLAN region firstly, and generate several reference points (RP). At each RP, the RSS values from all APs in the networks are calculated according to the concept of the combination of RTA and FDTD. As mentioned before, the modeling time is relatively long, especially in a larger area. To reduce the amount of computation, RPs are divided into two categories, namely C-RP (calculated RP) and E-RP (estimated RP). Only RPs labeled with C-RP will be input into the indoor modeling method, and corresponding RSS values are calculated and then obtained. Other RPs, referred as E-RPs, are considered as objectives with incomplete attribute(s), the RSS values of which are achieved through a data completing technique based on RST. As RST is a method with low complexity and processing overhead, the category of E-RP is the most important factor to reduce calculation. We take an example shown as Fig. 2 to clarify the concept of RPs in RST.

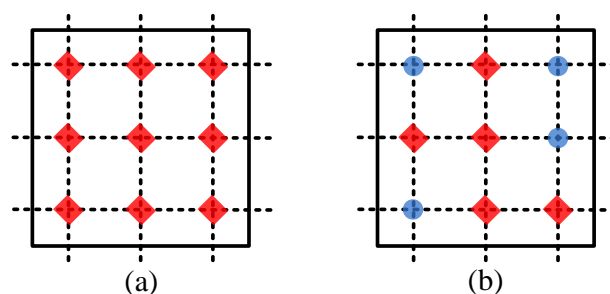


Fig. 2. Illustration of the relation amongst RPs, C-RPs and E-RPs.

In **Fig. 2(a)**, a WLAN region denoted by the outer square is meshed, and nine RPs represented by red diamonds are generated. Each RP is used to record RSS values, and the positioning procedure is executed amongst these points. As shown in **Fig. 2(b)**, RPs are divided into E-RPs (the four blue circles) and C-RPs.

To implement data completing for alleviating computation burden, rough set theory is introduced. RST is proposed by Pawlak as a type of data analysis theory. It is hypothesized that information systems only include precise (namely accurate and reliable) data, and any attribute of any object has an exclusive precise value; however, in reality the information systems are usually incomplete. In the proposed modeling method, the set consisting of C- and E-RPs can be considered as such an incomplete information system.

According to RST, an incomplete information system S can be defined as

$$S = \langle U, A, V, f \rangle \quad (7)$$

where U denotes the set of objectives (known as universe); A represents the attributes set of $U = \{x_1, x_2, \dots, x_n\}$; $V = \bigcup_{a \in A} V_a$, V_a denotes the range of an attribute a ; the mapping $f = U \times A \rightarrow V$ denotes the information function that determines the value of each attribute in U . Besides, $*$ is introduced to denote a missing value of an attribute. The similarity relation is introduced and expressed by

$$SIM = \left\{ \left((x_i, x_j) \mid x_i, x_j \in U \right. \right. \\ \left. \left. \wedge \forall a_k \left(a_k \in A \wedge \left(a_k(x_i) = a_k(x_j) \vee a_k(x_i) = * \vee a_k(x_j) = * \right) \right) \right) \right\} \quad (8)$$

where $i, j = 1, 2, \dots, n$ and $k = 1, 2, \dots, m$.

In an information system denoted by $S = \langle U, A, V, f \rangle$, supposing $a_j \in A$, the value range of which is $E_j = \{e_j^1, e_j^2, \dots, e_j^r\}$, and $x_t \in U$ is an objective, the probability of $a_j(x_t) = e_j^k$ can be considered as $\frac{1}{|E_j|}$ ($|E_j|$ is the number of elements in E_j). Therefore, for $x_t, x_s \in U$ and an attribute a_j , supposing $a_j(x_s) = e_j^k$, the probability that at the attribute a_j x_s is similar to x_t by the rule of SIM can be expressed by $P_j(x_s, x_t) = \frac{1}{|E_j|}$. Therefore, the probability that two objectives are similar by the rule of SIM at all the attributes can be expressed by

$$P(x_s, x_t) = \prod_{a_j \in A} P_j(x_s, x_t) \quad (9)$$

The similarity degree can be defined as

$$\mu(x_s, x_t) = \prod_{a_j \in A} P_j(x_s, x_t) \quad (10)$$

$R(i, j)$ is introduced to denote the element at the i -th row and j -th column in a similarity matrix, so R can be defined as

$$R(i, j) = \mu(x_i, x_j) \quad (11)$$

The data completing technique based on RST is as follows:

Input: the incomplete information system $S^0 = \langle U^0, A, V, f^0 \rangle$

Output: the complete information system $S = \langle U^r, A, V, f^r \rangle$

Step 1: Set $r = 1$.

Step 2: x_i and x_j denote any two objectives in $U^{r-1} \in S$, and calculate the similarity degree $\mu(x_i, x_j)$ by the rule of *SIM* to obtain the similarity matrix R^r .

Step 3: According to the line, scan and obtain the maximum value of $\mu(x_i, x_j)$ in R^r (except 0 and 1). If the number of the maximum value is greater than 1, the result is considered as the first one, which can be denoted by $R^r(p, q) = \mu(x_p, x_q)$, and $p, q = 1, 2, \dots, n$.

Step 4: Execute the following operations, revise S^{r-1} and obtain S .

Let $S^\# = S^{r-1}$.

(1) $k = 1$.

(2) **IF** $a_k(x_p) = *$ and $a_k(x_q) \neq *$, **THEN** $a_k(x_p) = a_k(x_q)$;

ELSE, IF $a_k(x_p) \neq *$ and $a_k(x_q) = *$, **THEN** $a_k(x_p) = a_k(x_q)$;

ELSE, IF $a_k(x_p) = *$ and $a_k(x_q) = *$, **THEN GOTO** (3).

(3) $k++$.

(4) **IF** $k \leq m$, **THEN GOTO** (2); **ELSE**, $r++$, **GOTO Step 5**.

Step 5: **IF** $S^r \neq S^\#$, **GOTO Step 2**; **ELSE**, **GOTO Step 6**.

Step 6: If there are any missing value in S^r , Friis free space equation is introduced to implement the data completing in this paper

$$a_k(x_j) = a_k(x_i) - 46 - 10n \cdot \log d_{i,j} \quad (12)$$

where $a_k(x_j)$ is the missing value, $a_k(x_i)$ is the value that $\mu(x_i, x_j)$ is maximum, and $d_{i,j}$ is the distance between x_i and x_j . n is the attenuation factor which differs in different environments. Generally, in the relatively isolated environment, the value of n is set between 3.0 and 3.5. According to the floor plan, with regard to the relatively less complexity of the given experiment environment, n here is set to 3 (it could be even lower if the internal partition is thin or soft).

Step 7: **IF** $S^r = S^\#$, **END**.

3.3 Evaluation

We employed the combination of ray-tracing and FDTD [11, 12] to model the floor where a research institution resides as shown in Fig. 3.

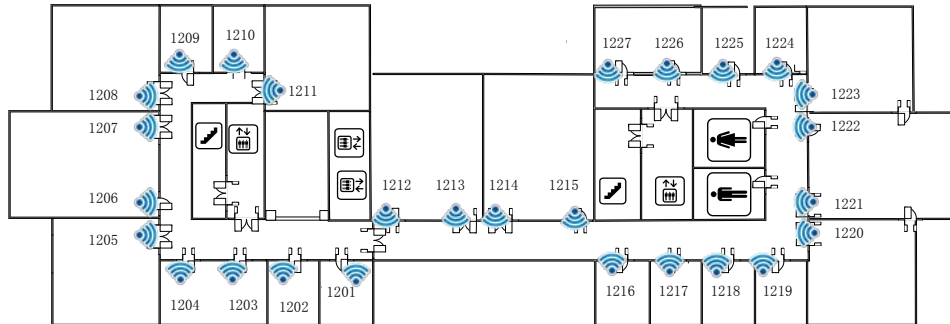


Fig. 3. The floor layout and AP deployment of offices, and the numbers denote doors.

To validate the model, we select some spots on our floor as RPs, measure and record values of Rx RSS at each RP as shown in Fig. 4, where the blue region is the interesting area and the right figure illustrates the partial details of the floor plan. With these sampled data a radio map thus can be built (the specific building details). Specifically, we receive and collect RSS actually is using a laptop (WLAN card build-in) with software 'Netstumbler', which is widely used for detecting and analyzing WLAN in 2.4GHz (802.11 /b/g/n). In addition, different APs may contribute differently to the positioning in the fingerprinting method as well. Two APs nearby, or the APs shared similar distance (LOS) to a nearby location point may contribute few (even do harm) to the positioning accuracy. It is exactly the reason that some researches (include our previous works) are concerning about the AP selection schemes to select most discriminating APs for positioning based on certain criteria, such as max mean, information entropy and joint entropy. In our case, we evenly deployed AP at each room of our research center, which are 27 APs in the whole positioning area as shown for providing both high AP density for positioning experiment and sufficient communication capacity for faculty staff or employee.

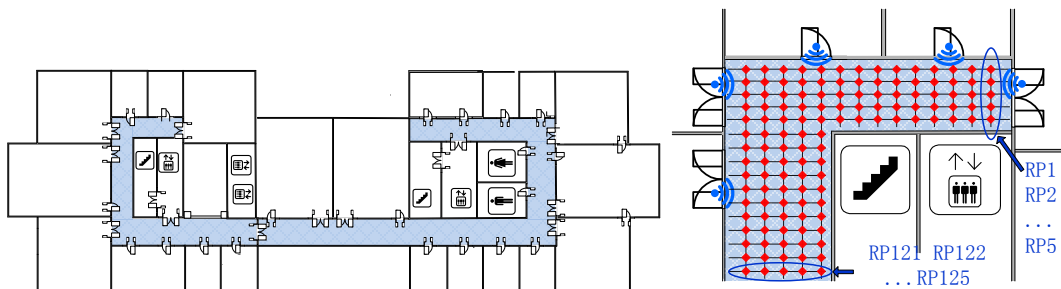


Fig. 4. Illustrations of RPs on corridors

For instance, Fig. 5 illustrates RSS at RPs received from the AP deployed in Room1202, where values of RSS are represented through different colors, and the AP is denoted by a solid blue triangle. As the constraint of authorization, RSS values are measured and recorded in 3 dedicated offices, and RPs are set unbalanced as all offices are furnished with tables, chairs, computers and other laboratory devices, which makes only sampling RPs in aisles are

available. On the contrary, in corridors, RPs are setup homogeneously with a 0.5 m sampling interval as shown in Fig. 5.

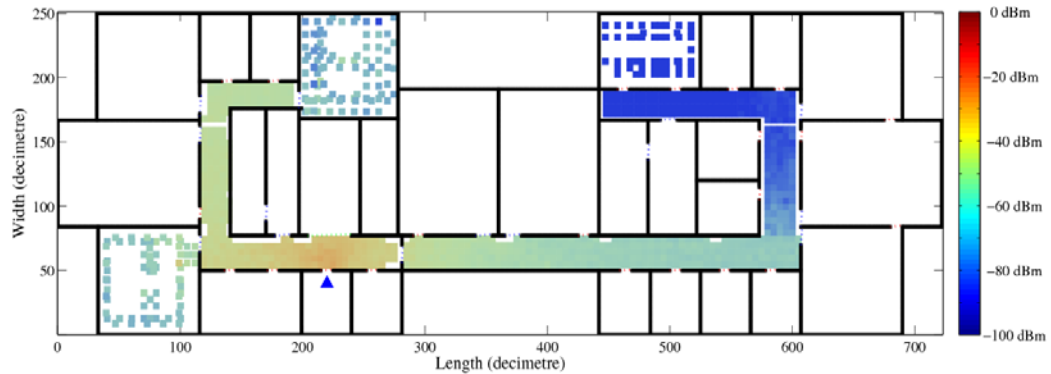


Fig. 5. Measured RSS at RPs from AP deployed in Room 1202 with a sampling interval of 0.5 m.

According to the investigation and discussion above, RSS at an arbitrary location on our floor from each AP can be estimated by the proposed method. To compare, RSS data on each location derived from AP in Room1202 are demonstrated as the example shown in Fig. 6.

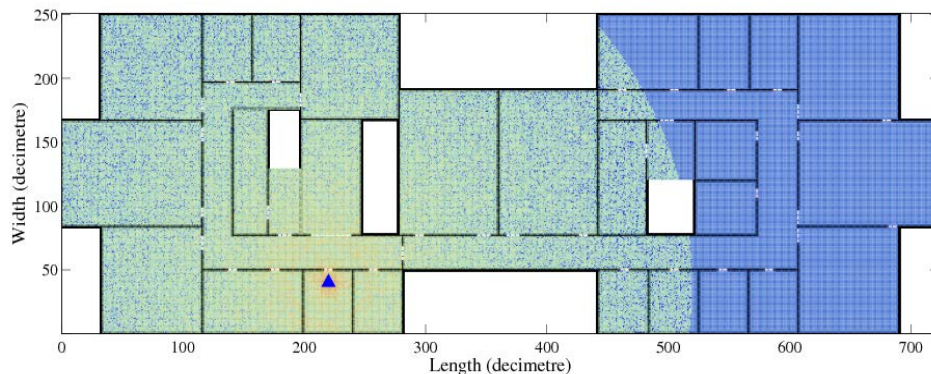


Fig. 6. Calculated RSS on our floor from AP deployed in Room1202 with a sampling interval of 0.1 m.

To be specific, RSS has been estimated at almost each location on our floor including all the offices, corridors, the hall, staircases and rest rooms, and the three blank areas denote elevator shafts where the network coverage is meaningless. It is worth noticing that the boundaries of dark blue, which denote values of RSS less than -80 dBm are arc-shaped. To reduce unnecessary calculation, we assumed that if the distance between an AP and a RP exceeds 30 m, the value of RSS at this RP from the AP is concerned as a value between -80 and -100 dBm, which is similar to the noise power setting in simulations, thus boundaries of RSS values less than -80 dBm present arc-shaped.

Comparison between measured RSS values and estimated counterpart from the AP in Room1202 is shown in Fig. 7 with different distances. According to the figure, measured RSS changes severely, particularly when RSS values are smaller. On the contrary, estimated RSS shows similar trend but is more stable. In addition, the estimating method could provide more RSS information. As the distance increases, the number of RPs share same distance is bound to escalate, and wave propagation between the AP to each RP becomes more complex due to

the fact that normally the amount of walls and doors need to be pass through may be variable. Owing to the diverse propagation environment, RSS in a small range might vary a lot, and the increased distance between AP and RP also would contribute to this phenomenon, which is proved by both blue and red curves of measured and calculated RSS in Fig. 7.

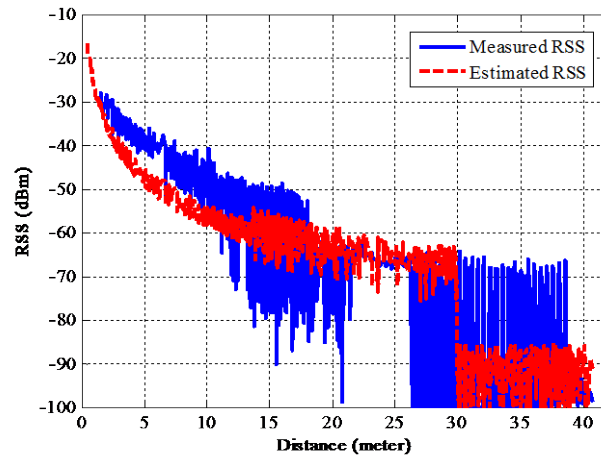


Fig. 7. Comparison of measured RSS and estimated results; RSS value is assigned between -90 and -100 dBm if the distance between RP and AP exceeds 30m for reducing unnecessary calculation.

In this paper, to reduce the calculation burden, RPs are divided into C-RPs (calculated RP) and E-RPs (estimated RP), between which the C-RP is for the indoor propagation model as input, and the RSS value of the E-RP is obtained by RST. To employ RST, an incomplete information system needs to be generated firstly, in which RPs are considered as objectives, and physical location information of RPs is considered as the attributes of objectives. Locations amongst generated RPs are different, due to the *SIM* eq.(8) regulation between two RPs is represented by the similarity relation. Thus, the actual physical location information is ill-suited in this case. Therefore, we introduce three parameters to transform the absolute information into several relative information categories. The first attribute is the label of areas, to achieve which we further partition the WLAN region.

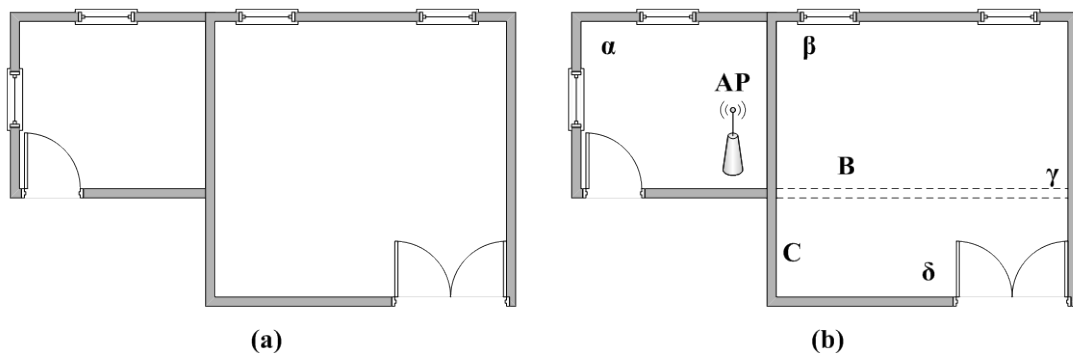


Fig. 8. An example of the way to further partition the WLAN region.

Fig. 8 is an illustration of region partition. To be specific, Fig. 8(a) shows the original region (not partitioned yet), which consisting of two rooms. To further partition the region, the actual walls need to be virtually prolonged, and form several areas that are surrounded by

actual walls, actual & virtual walls, or only by virtual walls. In **Fig. 8(b)**, after virtually prolonging the walls, four areas (denoted by α , β , γ and δ) are distinguished. Partition attributes of RP labeled B and C in **Fig. 8(b)**, therefore, are β and δ , respectively.

The second attribute is the fuzzy distance between the current RP and the corresponding AP rather than the true distance. As the WLAN is meshed and several RPs are generated, if the average interval amongst RPs are l , the fuzzy distance d^* can be defined as

$$d^* = \text{round}(d/l) \quad (13)$$

where d is the true distance, $\text{round}(\bullet)$ denotes the operator to rounding.

The third attribute derived from the physical location is the number of obstacles (we mainly consider it as walls for simplicity, which are built with same material) between a RP and an AP, which are 1 and 2 for RP B and C in **Fig. 8(b)**. We define RSS values at each RP from an AP as the last attribute, which are known at C-RPs and unknown at E-RPs, so the incomplete information system is obtained.

The scale of E-RPs and C-RPs significantly affects the accuracy of the data completing system. To generate the information system, RSS data of AP in Room1202 are introduced as the completing information system. C-RPs are chosen from RPs in different proportion, the RSS values of E-RPs are obtained through RST, and the results are shown in **Fig. 9**.

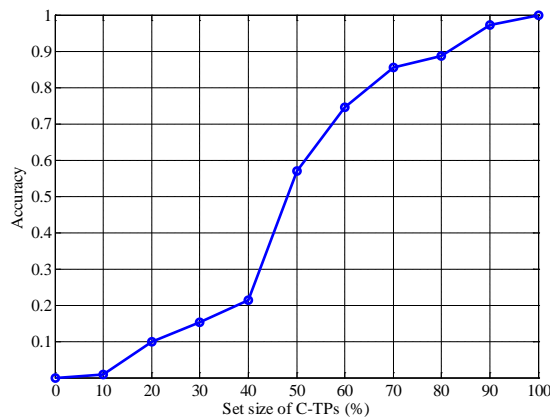


Fig. 9. Accuracy of the data completing system under different conditions

It is illustrated that the data accuracy decreases along with more E-TPs taking part in. For instance, if set size of C-RPs is 60% (40% E-TPs size), the accuracy could be over 75%, which is reasonable in terms of a fingerprinting dataset. In this case, approximately 40% of the computational burden can be reduced.

4. Improvement of Indoor Propagation Analysis Approach with the Factor of Moving People and Corresponding Application in the indoor Positioning System

The radio map generated either through measurement or simulation usually takes no time-varying characteristic into account. In fact, besides the infrequent facility-moving and infrastructure-changing, constantly moving crowd may greatly change the propagation environment. Our measured data base is built in a relatively ideal environment where few people move around and all doors and windows are closed. And the simulated one is also calculated without considering the factor of moving people. Nevertheless, people in a RF environment may affect the RF signals for a wide range of frequencies [26,27], including the 2.4 and 5 GHz bands common in Wi-Fi networks. Therefore, in order to obtain more accurate positioning information, the factor of moving people is introduced into the radio map data base in our proposed system.

4.1 The Factor of Moving People

Due to spatial and temporal dependency of RSS values, the factor of moving people is taken into consideration when building or updating a radio map. Both in [26] and [27], the influence of human traffic is studied through measurement. Moreover, in [26], an empirical equation and the way of iteration are given. Firstly, the average power loss for different frequency responses (or Root Mean Square) delay spread for different impulse responses is obtained. Then, we consider the Euclidean distance between a reference frequency/impulse response and each response recorded during the day. The reference response is calculated as the average of the first N responses recorded during the night (0-8 h):

$$r = [r(1), r(2), \dots, r(n)] = \frac{1}{N} \sum_{k=1}^N [x_k(1), x_k(2), \dots, x_k(n)] \quad (14)$$

With this reference response, the normalized Euclidean distance between a response $\mathbf{x}_k = [x_k(1), x_k(2), \dots, x_k(n)]$ can be obtained as

$$d(\mathbf{x}_k, r) = \sqrt{\frac{1}{n} \sum_{i=1}^n [x_k(i) - r(i)]^2} \quad (15)$$

According to the study in [27], when analyzing the relations between RSS and human traffic, the parameter $d(\mathbf{x}_k, r)$ can be considered as the power loss on average. Referring to the reference responses, the RSS results without moving people are qualified candidates.

In the given offices, we selected several RPs, at which the conditions of moving people and RSS values were recorded during a whole week, and results are shown in Fig. 10. Both people moving and average RSS value on RPs differed a lot between week days and weekends, hence, the results of measurement are demonstrated in regional average respectively, where the color bar represents the normalized value of moving people. Specifically, in the experiment, we selected several RPs along with the corridor, on which we recorded the number of individuals went through the point and the RSS values of the point. After one week collection and measurement, we did the statistics. The number of moving peoples was normalized and averaged in the process, and then those RPs shared similar numbers of moving peoples were assigned together and formed the regions, which is demonstrated in the Figure below with labels from 1 to 6. For instance, region 1 is the part of corridor near the store room (the square on the right of region 1) and two office rooms where the two professors were occasionally on business. So the normalized moving people factor is few as indicated in color bar. As the contrast, students and staff frequently went through the region 4, where near both the entrance of elevators and the lab. Therefore the factor of moving people there was about 0.7.

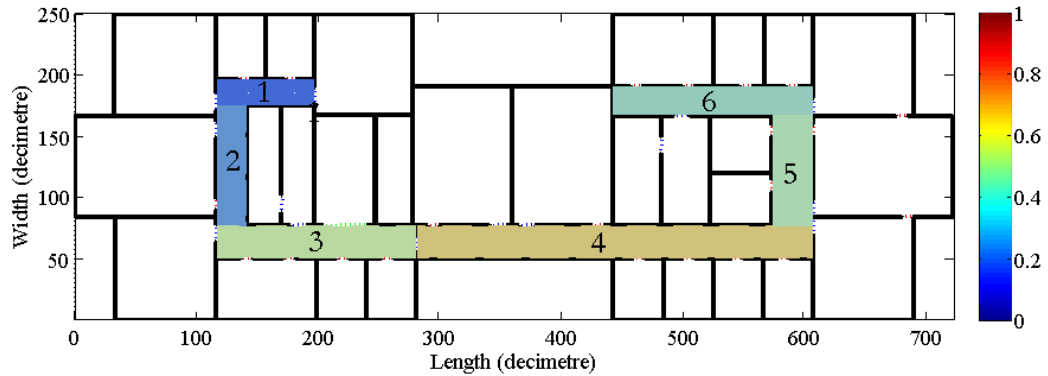


Fig. 10. The average human traffic in the office environment during a week

Moreover, RPs near the exit of the layout is most typical because the human traffic is relatively high. Therefore, the fluctuation of moving people during the week and weekend days near the exit are illustrated in **Fig. 11**.

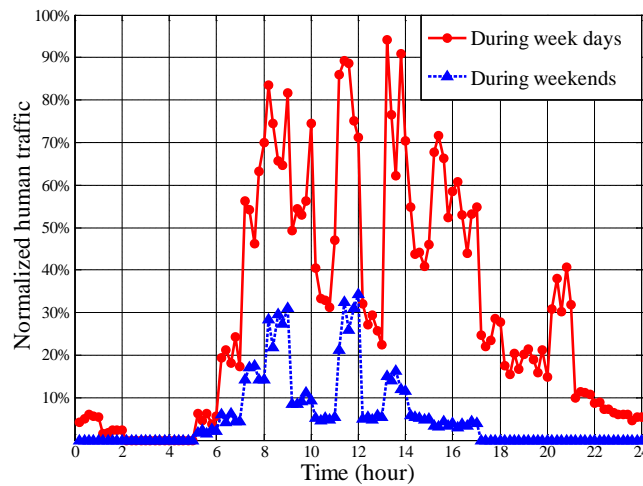


Fig. 11. The human traffic recorded near the exit during week and weekend days respectively.

Specifically, the solid and dotted lines denote the situations of human traffic during week and week-end days, respectively. And values of traffic are normalized with the maximum value in a week. To show the influence due to the traffic, we record RSS values at selected RPs in a week as well. For illustration, the RSS values received from AP deployed in Room 1201 is taken as an example, which is shown in **Fig. 12**.

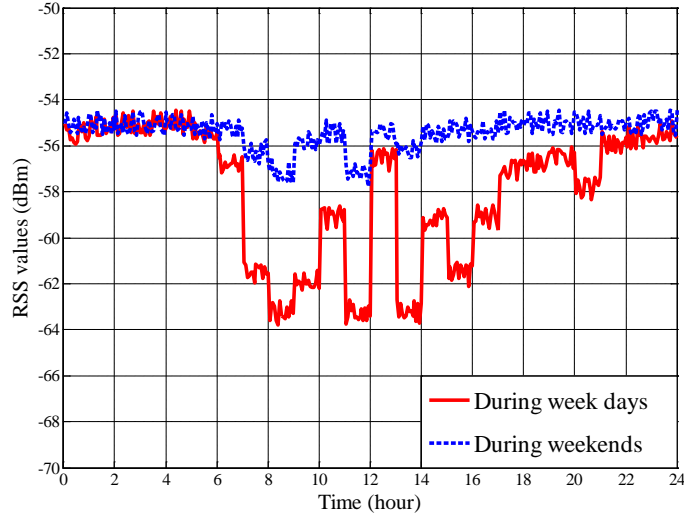


Fig. 12. Temporal measurements of RSS value received from AP deployed at selected RPs near the exit.

As shown in **Fig. 12**, the human traffic significantly affects the RSS values. The indoor positioning system implemented in our previous work [9, 10] is a type of finger printing method, the positioning results of which at last are achieved through matching the data in the radio map and the actual received RSS values. Therefore, the fluctuation is critical to the positioning accuracy. This issue, however, is not addressed by most researches in the indoor positioning system.

In this paper, we introduce the factor to the indoor positioning system as an important supplement. First, the situation of human traffic and corresponding RSS values for parts of RPs are recorded, and \mathbf{x}_k in (15) can be achieved, and hence, the relations between the location and RSS values can be expressed as a time-depending function.

At time t , if a specific location is denoted by x and the RSS received at this RP is denoted by RSS , RSS can be achieved by

$$\arg \max P(RSS|x) = \arg \max P(RSS|d(\mathbf{x}_k, r)) \quad (16)$$

Thus, given a location, the corresponding RSS values can be obtained by maximizing (16).

4.2 The New Approach for the Radio Map Updating and the brief Introduction of the Proposed Indoor Positioning System

In this paper, the radio map is built through a simulation method, which consists of RTA, FDTD and RST, and possesses time-depending reliability. To be specific, the temporal feature is introduced due to the change of human traffic over time. Therefore, in the new radio map data system, a time-depending factor is introduced as well, which is mainly based on the typical models of human traffic. For instances, a radio map in terms of a day includes 360 radio maps in terms of every 15 minutes, and a radio map in terms of a week includes seven radio maps in terms of a day. Moreover, data during holidays are well distinguished. In each radio map, the data is generated based on the indoor propagation and penetration analysis. To reduce the amount of calculation, RST improves the time efficiency at a slight expense of the

positioning accuracy. In RST, RPs are divided into C-RPs and E-RPs, where actually the loss of accuracy is mainly due to the E-RPs.

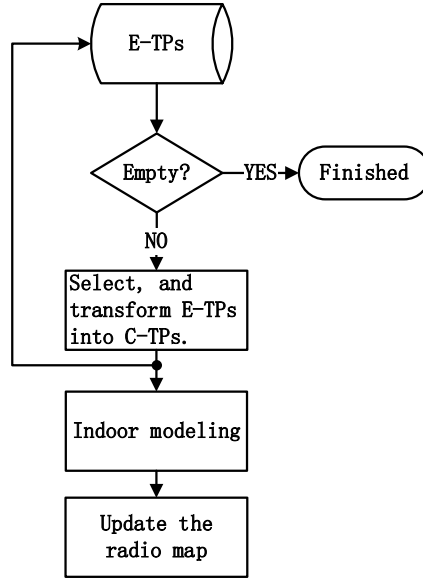


Fig. 13. The updating procedure for radio maps.

In the implementation of updating for radio map, the amount of E-RPs decreases gradually, and E-RPs turn to be C-RPs. This procedure is shown in **Fig. 13**. The updating approach consists of two components, which are generating time-dependent radio maps and making radio maps fully based on the combination of RTA and FDTD. As the development of hardware, the radio map can be built purely through FDTD in future.

In our previous work [9, 10], an indoor positioning system is proposed, which is a type of fingerprinting method, and the corresponding data are obtained through manual measurement. To be specific, fingerprinting method has been widely deployed and developed in many indoor location systems [28-30], a typical fingerprinting indoor positioning system is firstly introduced as follows. As long as an end user takes RSS readings from available APs with his/her (WLAN adapter equipped) device in an indoor environment, the positioning system then could estimate the current location of the user based on the measured RSS value by matching this RSS value with the fingerprint database, which is the pre-stored table of RSS values over a grid of reference points (both RSS values and location coordinates of the reference points are recorded) on the positioning area. Therefore, as shown in **Fig. 14** the fingerprinting method mainly consists of two parts, which are radio map building and the RSS matching procedures, in the offline phase and online phase respectively.

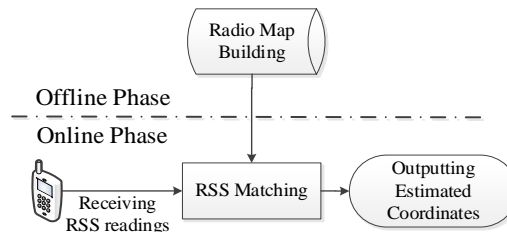


Fig. 14. Traditional Fingerprinting Indoor Positioning System

1) Radio map is a dataset used for matching RSS with position. Based on numerous Reference Points (RPs) where both the RSS value and location are known, we may statistically represent the electromagnetic environment of the interesting area and implement the positioning process. An original radio map normally consists of two parts, which are RSS value and coordinate. We denote the RSS values derived from AP i at RP j as $\phi_{i,j}$. So the radio map of RSS part is denoted as Φ :

$$\Phi = \begin{bmatrix} \phi_{1,1} & \phi_{1,2} & \dots & \phi_{1,M} \\ \phi_{2,1} & \phi_{2,2} & \dots & \phi_{2,M} \\ \vdots & \vdots & \dots & \vdots \\ \phi_{N,1} & \phi_{N,2} & \dots & \phi_{N,M} \end{bmatrix} \quad (17)$$

where M and N stand for the total number of available APs and RPs respectively. Therefore each row of Φ , the vector of the matrix, actually represents the RSS values of each RP, which is denoted as:

$$\phi_j = [\phi_{j,1}, \phi_{j,2}, \phi_{j,3}, \dots, \phi_{j,M}], j = 1, 2, \dots, N \quad (18)$$

Then, the radio map can be denoted as (P_{xy}^j, ϕ_j) , $j = 1, 2, \dots, N$, $\phi_j \in \mathbb{R}^M$, where the element P_{xy}^j is the coordinates of the RP j , which is represented by (x_j, y_j) . In the case of no RSS readings can be received from an AP at RPs, a minimal value will be set for subsequent algorithm computation.

2) We take Weight K-Nearest Neighbors (WKNN) algorithm as the matching process in the proposed positioning system for simplicity and low complexity. Although many algorithms are widely used in fingerprinting method for matching the RSS of the location point with the radio map, including Kernel Method, probabilistic approach, Support Vector Regression (SVR) and Neural Network [28].

Specifically, a group of RSS readings is sampled by a terminal, and then it is matched with the most likely location by traversing all RPs of the radio map. For measuring the similarity between location point and each RP, KNN algorithm calculates the distances between the location point and each RP by:

$$D_i = \left(\sum_{j=1}^M \|\phi_{test,j} - \phi_{i,j}\|^2 \right)^{\frac{1}{2}}, i = 1, 2, \dots, N, j = 1, 2, \dots, M \quad (19)$$

where the RSS values derived from AP j at RP i is $\phi_{i,j}$, $\phi_{test,j}$ is the received RSS value from AP j at location point, M and N stand for the total number of available APs and RPs respectively, D_i is the Manhattan distance between the location point and the RP i . The first K RPs (we set the K as 4 in the system) with the shortest distance are chosen to estimate the location of the point, so the output coordinates of the location point can be given by:

$$P_{xy}^{test} = \frac{1}{\zeta} \sum_{\zeta=1}^{\zeta} P_{xy}^{\zeta}, \zeta = 1, 2, \dots, K \quad (20)$$

where the P_{xy}^{ζ} is the coordinates of the RP ζ , which is recorded in the radio map as the known quantities (the applied WKNN method is as same as the KNN method, except the final step where we use normalized weight based on distance to calculate coordinates instead of using the average).

It is obvious that the dimensionality of a radio map depends on both the number of RPs and quantity of deployed APs. Therefore, in the case of positioning a quite large area with many RPs needs to be set and numerous APs are required for dense coverage, so the size of radio

map will be expanded considerably and the computational burden will be increased sharply. Besides, in case of some APs are broken down, the fingerprinting system may be severely damaged or even malfunction due to the missed dimension.

Our former works therefore focused on those issues and proposed several solutions, which are radio map division for narrowing searching space and feature extraction algorithm for reducing the dimension of the radio map. For the specific steps we have cited flow chart shown in Fig. 15 and made the reference [9]. In this article, we solely dedicated to the radio map building portion, therefore the radio map division and feature extraction procedures actually have no influence on the positioning performances comparison, since both the systems (the one in our previous work and the one in this manuscript, respectively) deployed the same positioning scheme.

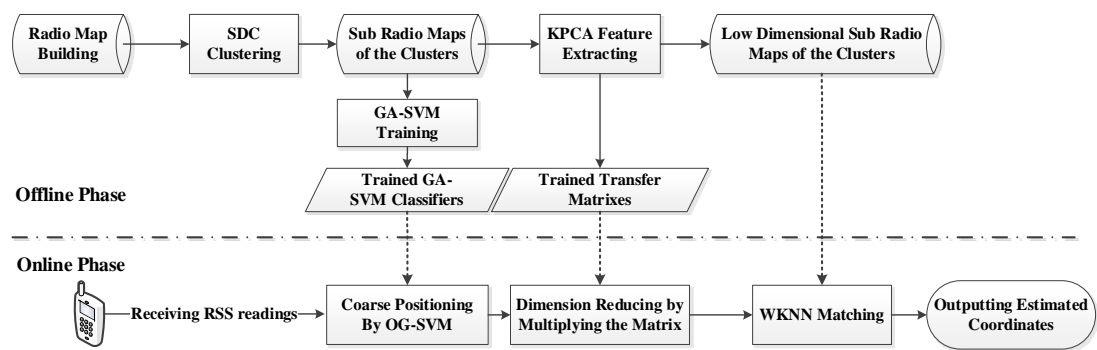


Fig. 15. Flow chart of the proposed indoor positioning system.

In this paper, we maintain the main working mechanism of this system, and replace the module of ‘radio map building’ with the new data base achieved by the proposed radio map building and updating approach. In another word, the human traffic effect functions on the ‘Radio Map Building’ procedure, which is shown in the upper block in the Fig. 14 for traditional fingerprinting system as well as in the first block in the Fig. 15 for the proposed system. Based on the equation (16), groups of RSS values in the radio map are updated and recorded according to the human traffic factor in the area during the certain time period. The online positioning procedure then will be conducted based on the dynamic radio maps as illustrated before.

4.3 Evaluation

In [9] and [10], the performance of our previous positioning system has been proven, and the feasibility and reliability of the proposed system have been validated in Android OS based smart terminal. In this paper, a building and updating method for the radio map is introduced, the evaluation of which is implemented through the comparisons between the previous (original) and improved systems.

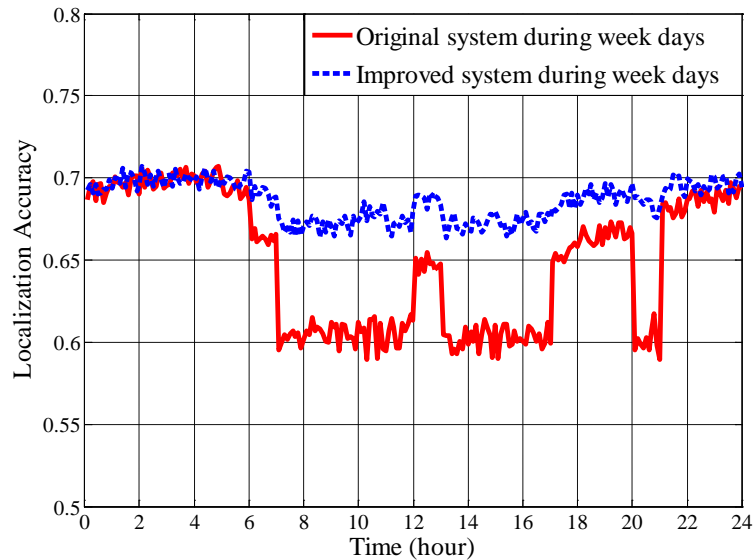


Fig. 16. Confidence probability comparison between previous system and enhanced system during week days.

As mentioned before, the original radio map was built during the summer vacation, when human traffic is extremely low. Hence, the corresponding radio map is appropriate for weekends or late night of week days, during those periods the traffic is low as well. In the specific regions denoted in [Fig. 10](#), we deploy several terminals and run the positioning systems for a week. We recorded and compared the positioning results of the two systems every ten minutes. To illustrate, we select the results obtained from the top left region, and distinguish the results according to sampling period which are week and week-end days respectively. The comparisons of the positioning accuracy are conducted within 1 meter. To be specific, we selected many locations and collected RSS values as the test points, on which we ran the positioning system and received the estimated location coordinates accordingly. For each estimated location, we compared it with the corresponding test point and calculated the distance in between. For those estimated results where distances is within 1 meter, we counted it as the numerator of the positioning accuracy, while the total number of the test points was the nominator. [Fig. 16](#) illustrates the comparison results between the systems proposed in our previous work and in this paper during week days. According to the human traffic shown in [Fig. 11](#), the confidence probability of the original system is roughly same as the improved system during idle hours. However, it fluctuates significantly during the working hours when human traffic is relatively high, the positioning accuracy decreases to approximately 60%. On the contrary, the improved system can nearly maintain the accuracy due to the introducing of the updating method used for the radio map.

[Fig. 17](#) shows the comparison results during weekends. As the current traffic normally is lower in holidays, the fluctuation of accuracy in the original system alleviates notably. It clearly demonstrates that the confidence probability achieved through the original system has significant relationship with the human traffic. In other words, the original system takes less consideration about the factor of environment variables, which makes the actual availability poor, as the most typical application scenarios of the indoor positioning system are the shopping malls and conference center, where the moving crowd heavily depends on different

date. In the contrast, the confidence probability of the improved system is much more stable, it is due to the features of the updating method proposed in this paper.

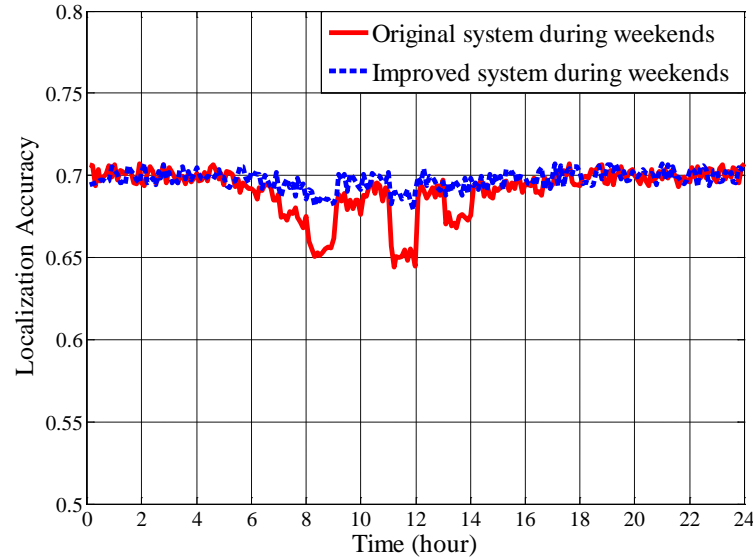


Fig. 17. Confidence probability comparison between previous system and enhanced system during weekends.

As the radio map in the original system is measured during summer vacation when human traffic is extremely low, hence, the features of received signals are more similar with the data during late nights in week days, which explains the fact that the original system performs similar with the new one during night and idle hours, especially in weekends. However, the status is different in rush hours, when most people actually require and use the location based service. It demonstrates that the spatial and temporal dependency of the radio map is strong, which means the influence caused by moving people should be reasonably considered.

In regards to the complexity comparison with the conventional fingerprinting system, we have addressed the related issue in our previous works. Specifically, in the offline phase, for the original system or traditional fingerprinting system, we collected the radio map by measurements, which in fact took 12 people nearly two weeks (5 hours per day) to sample the RSS values and build it with laptops. For the improved system, based on the proposed method, we may build it by powerful simulation system according to the floor plan, which is apparently much more labor-saving and efficient. For the online phase, computational complexity of the OG-SVM is $O(Cn_{sv})$, where C is the number of classes and n_{sv} is the number of support vectors. The counterpart of KPCA is $O(dMN)$, where d is the number of the (reduced) low dimensionality, M is the number of features (APs) and N is the number of reference points. Therefore the computational complexity of the proposed positioning system is $O(dMN)$ plus $O(dN)$ and $O(Cn_{sv})$, while the computational complexity of conventional fingerprinting method is $O(MN)$. Therefore, the deployed system indeed caused more computational complexity than the conventional method. Nevertheless, considering the contribution of enhancing robustness and reducing storage of the radio map, the proposed system is still effective and reasonable.

5. Conclusion

In this paper, we propose an updating technique for radio maps used in the indoor positioning system. The method includes the indoor propagation and penetration modeling and the analysis of human traffic. The approach of indoor propagation modeling reflects the spatial dependency of the radio map, and based on the combination of RTA, FDTD and RST, in which RTA is introduced to reduce the vast calculation of FDTD, and RST is employed for further decrease. To reflect the temporal dependency, we study and implement the factor of moving people. With measurement and statistics, the factor of human traffic is introduced as the temporal updating component. At different time points, different radio maps can be applied. With these time-dependent radio maps we build a comprehensive data base used for indoor positioning, i.e. we introduce the updating method into the positioning system proposed in our previous works, and implement the corresponding application. In other words, actually we do not improve the system positioning accuracy by optimization, but focus on the weak point of the system and boost the performance in average (or in terms of a long period) by reducing the human traffic influence. Finally, we compare the results between the original and improved systems. The results show that the original system severely suffers the fluctuation of human traffic, which lead to poor availability during rush hours. However, our improved system effectively lowers the influence caused by moving people, and the positioning accuracy relatively maintains stable during week and weekend days.

References

- [1] H. Yucel, T. Ozkir, R. Edizkan, A. Yazici, "Development of indoor positioning system with ultrasonic and infrared signals," in *Proc. of International Symposium on Innovations in Intelligent Systems and Applications*, vol. 1, pp. 2-4, 2012. [Article \(CrossRef Link\)](#)
- [2] Z.L. Deng, Y.P. Yu, X. Yuan, N. Wan, and L. Yang, "Situation and development tendency of indoor positioning," *China Communications*, vol. 10, no. 3, pp. 42-55, 2013. [Article \(CrossRef Link\)](#)
- [3] M. Raitoharju, T. Fadjukoff, S. Ali-Loytty, and R. Piche, "Using unlocated fingerprints in generation of WLAN maps for indoor positioning," in *Proc. of Position Location and Navigation Symposium*, pp. 23-26, 2012. [Article \(CrossRef Link\)](#)
- [4] L. Wirola, T.A. Laine, and J. Syrjarinne, "Mass-Market Requirements for Indoor Positioning and Indoor Navigation," in *Proc. of IEEE Indoor Positioning and Indoor Navigation*, pp.1-7, 2010. [Article \(CrossRef Link\)](#)
- [5] P. Bahl and V. Padmanabhan, "Radar: An in-building RF-based user location and tracking system," in *Proc. of IEEE Conference on Computer Communications*, pp. 775-784, 2000. [Article \(CrossRef Link\)](#)
- [6] Y. Ji, S. Biaz, S. Pandey, and P. Agrawal, "Ariadne: a dynamic indoor signal map construction and localization system," in *Proc. of 4th international conference on Mobile systems, applications and services*, pp. 151-164, 2006. [Article \(CrossRef Link\)](#)
- [7] T. P. Deasy and W. G. Scanlon, "Simulation or measurement: The effect of radio map creation on indoor wlan-based localisation accuracy," *Wireless Personal Communications*, vol. 42, no. 4, pp. 563-573, 2007. [Article \(CrossRef Link\)](#)
- [8] K. Chintalapudi, A. Padmanabha Iyer, and V. N. Padmanabhan, "Indoor localization without the pain," in *Proc. of Sixteenth Annual International Conference on Mobile Computing and Networking*, pp. 173-184, 2010. [Article \(CrossRef Link\)](#)
- [9] Y. Mo, Z. Zhang, Y. Lu, W. Meng, M. Lin, W. Yao, "A Spatial Division Clustering Method and Low Dimensional Feature Extraction Technique Based Indoor Positioning System," *Sensors*, vol.14, no. 1, pp. 1850-1876, 2014. [Article \(CrossRef Link\)](#)

- [10] Y. Mo, Z. Zhang, Y. Lu, W. Meng, G. Agha, "Random Forest Based Coarse Locating and KPCA Feature Extraction for Indoor Positioning System," *Mathematical Problems in Engineering*, vol. 2014, Article ID 850926, 8 pages, 2014. [Article \(CrossRef Link\)](#)
- [11] Y. Lu, X. Tan, Y. Mo, L. Ma, "A new green clustering algorithm for energy efficiency in high-density WLANs," *KSII Trans. on Internet and Information Systems*, vol. 8, no. 2, pp. 326-354, 2014. [Article \(CrossRef Link\)](#)
- [12] Y. Lu, X. Tan, Y. Mo, L. Ma, "Green clustering implementation based on DPS-MOPSO," *Mathematical Problems in Engineering*, vol. 2014, article ID. 721718, pp. 1-13, 2014. [Article \(CrossRef Link\)](#)
- [13] Y. Kim, Y. Chon, H. Cha, "Smartphone-based collaborative and autonomous radio fingerprinting," *IEEE Trans. on Systems, Man and Cybernetics*, vol. 24, no. 1, pp. 112-122, 2012. [Article \(CrossRef Link\)](#)
- [14] M. Raspopulos, C. Laoudias, L. Kanaris, A. Kokkinis, C.G. Panayiotou, S. Stavrou, "3D ray tracing for device-independent fingerprint-based positioning in WLANs," *Positioning Navigation and Communication*, vol. 109, no. 113, pp. 15-16, 2012. [Article \(CrossRef Link\)](#)
- [15] L. Ni, Y. Liu, Y. C. Lau, and A. Patil, "Landmarc: indoor location sensing using active RFID," in *Proc. of IEEE International Conference on Pervasive Computing and Communications*, pp. 407-415, 2003. [Article \(CrossRef Link\)](#)
- [16] P. Krishnan, A. Krishnakumar, W.H. Ju, C. Mallows, and S. Gamt, "A system for lease: location estimation assisted by stationary emitters for indoor RF wireless networks," in *Proc. of IEEE Conference on Computer Communications*, vol. 2, pp. 1001-1011, 2004. [Article \(CrossRef Link\)](#)
- [17] J. Yin, Q. Yang, and L. Ni, "Learning adaptive temporal radio maps for signal-strength-based location estimation," *IEEE Trans. on Mobile Computing*, vol. 7, no. 7, pp. 869-883. 2008. [Article \(CrossRef Link\)](#)
- [18] Z. Sun, Y. Chen, J. Qi, and J. Liu, "Adaptive localization through transfer learning in indoor Wi-Fi environment," in *Proc. of Seventh International Conference on Machine Learning and Applications*, pp. 331-336, 2008. [Article \(CrossRef Link\)](#)
- [19] S. Sorour, Y. Lostonlen, S. Valaee, "Reduced-effort generation of indoor radio maps using crowdsourcing and manifold alignment," in *Proc. Of Sixth International Symposium on Telecommunications*, pp. 354-358, 2012. [Article \(CrossRef Link\)](#)
- [20] J.S. Lim, W.H. Jang, G.W. Yoon, D.S. Han, "Radio map update automation for WiFi positioning systems," *IEEE Comm. Letters*, vol. 17, no. 4, pp. 693-696, 2013. [Article \(CrossRef Link\)](#)
- [21] W. Liu, B.Q. Ng, B. Liu, Y.L. Guan, Y.H. Leow, J. Huang, "Radio map position inference algorithm for indoor positioning systems," in *Proc. of IEEE International Conference on Networks*, vol. 161, no. 166, pp. 161-166, 2012. [Article \(CrossRef Link\)](#)
- [22] C.Y. Shih, L.H. Chen, G.H. Chen, E.H.K Wu, M.H Jin, "Intelligent radio map management for future WLAN indoor location fingerprinting," in *Proc. of IEEE Wireless Communications and Networking Conference*, pp. 2769-2773, 2012. [Article \(CrossRef Link\)](#)
- [23] M. Thiel, and K. Sarabandi, "A hybrid method for indoor wave propagation modeling," *IEEE Trans. on Antennas and Propagation*, vol. 56, no. 8, pp. 2703-2708, 2008. [Article \(CrossRef Link\)](#)
- [24] Y. Wang, S. Safavi-Naeini, and S. K. Chaudhuri, "A hybrid technique based on combining ray tracing and FDTD methods for site-specific modeling of indoor radio wave propagation," *IEEE Trans. on Antenna Propagation.*, vol. 48, no. 5, pp. 743-754, 2000. [Article \(CrossRef Link\)](#)
- [25] Y. Wang, S. K. Chaudhuri, and S. Safavi-Naeini, "An FDTD/ray-tracing analysis method for wave penetration through inhomogeneous walls," *IEEE Trans. on Antenna Propagation*, vol. 50, no. 11, pp. 1598-1604, 2002. [Article \(CrossRef Link\)](#)
- [26] G. Zaharia, G. Zein, and J. Citerne, "An experimental investigation of the influence of the moving people on the indoor radio propagation," in *Proc. of Antennas and Propagation Society International Symposium*, vol. 3, pp. 1898-1901, 1994. [Article \(CrossRef Link\)](#)
- [27] P. Hafezi, A. Nix, and M.A. Beach, "An experimental investigation of the impact of human shadowing on temporal variation of broadband indoor radio channel characteristics and system performance," in *Proc. of IEEE 52nd Vehicular Technology*, vol. 1, pp. 37-42, 2000. [Article \(CrossRef Link\)](#)

- [28] S.H. Fang and T.N. Lin, "Indoor Location System Based on Discriminant-Adaptive Neural Network in IEEE 802.11 Environments," *IEEE Trans. on Neural Networks*, vol.19, no.11, pp.1973-1978, 2008. [Article \(CrossRef Link\)](#)
- [29] C. Steiner, A. Wittneben, "Low Complexity Location Fingerprinting With Generalized UWB Energy Detection Receivers," *IEEE Trans. on Signal Processing*, vol. 58, no. 3, pp.1756-1767, 2010. [Article \(CrossRef Link\)](#)
- [30] T.N. Lin; P.C. Lin, "Performance comparison of indoor positioning techniques based on location fingerprinting in wireless networks," in *Proc. of International Conference on Communications and Mobile Computing Wireless Networks*, vol. 2, pp. 1569-1574, 2005. [Article \(CrossRef Link\)](#)



Yun Mo received the B.S. degree from Beijing Technology and Business University, Beijing, China, in 2009, and the M.S. degree from University of Melbourne, Melbourne, Australia in 2011, respectively. He is working toward the Ph.D. degree with the School of Electronics and Information Engineering, Harbin Institute of Technology. He currently continues his research in Open System Laboratory, University of Illinois at Urbana-Champaign, USA as Visiting Scholar. His current research interests include machine learning, indoor positioning and navigation.



Zhang Zhongzhao (M'96) received the B.S. degree in wireless communication from Heilongjiang University, Harbin China, in 1981 and the M.S. degree in communication engineering from Harbin Institute of Technology (HIT), Harbin China, in 1984. He was a full professor with wireless communication in 1992 and Dean of Institute of Electronics and Information Engineering, HIT, from 2003-2012. Since 2001, he has been the Director of the Communication Research Center, HIT. He has published 5 books and over 190 papers for journals and international conferences. His research interests include mobile communication, wireless communication and satellite communication. Prof. Zhang is a Fellow of China Institute of Communication, the Chairman of Heilongjiang Institute of Electronics. He received 2 second- and 2 third-class awards from the China national science and technology progress.



Yang Lu received his B.S. and M.S. in information and communication engineering from Harbin Institute of Technology, Harbin, China, in 2007 and 2011, respectively. He has achieved the Ph.D. degree in School of Electronics and Information Engineering, Harbin Institute of Technology in 2015 and is currently working at Huawei Technology Co. Ltd in Shanghai. His research interests include energy efficient strategy in high-density wireless LANs and networking technology in cognitive radio.



Gul Agha is Professor of Computer Science at the University of Illinois at Urbana-Champaign. Dr. Agha is a Fellow of the IEEE. He served as Editor-in-Chief of *IEEE Concurrency: Parallel, Distributed and Mobile Computing* (1994-98), and of *ACM Computing Surveys* (1999-2007). He has published over 200 research articles and supervised 30 PhD dissertations. His book on Actors is among the most widely cited in concurrent and distributed computing. Besides work on semantics and implementation of actor languages, Agha's research group has developed novel coordination languages, methods for software testing (including concolic testing), computational learning for verification, statistical model checking, and Euclidean model checking. In collaboration with Civil Engineers, he has developed methods for autonomic structural health monitoring (SHM) of civil infrastructure using wireless smart sensor networks. Dr. Agha is a co-founder of Embedor Technologies, a company providing solutions for infrastructure monitoring in smart cities.